

This article was downloaded by:

On: 23 January 2011

Access details: *Access Details: Free Access*

Publisher *Taylor & Francis*

Informa Ltd Registered in England and Wales Registered Number: 1072954 Registered office: Mortimer House, 37-41 Mortimer Street, London W1T 3JH, UK



Journal of Coordination Chemistry

Publication details, including instructions for authors and subscription information:

<http://www.informaworld.com/smpp/title~content=t713455674>

Hydrothermal synthesis and crystal structures of two new divalent metal phosphonates with layered structure

Lei Meng^a; Zhengang Sun^a; Dapeng Dong^a; Hui Chen^a; Yanyu Zhu^a; Jing Zhang^a; Yan Zhao^a; Wansheng You^a

^a Faculty of Chemistry and Chemical Engineering, Institute of Chemistry for Functionalized Materials, Liaoning Normal University, Dalian, P. R. China

First published on: 29 June 2007

To cite this Article Meng, Lei , Sun, Zhengang , Dong, Dapeng , Chen, Hui , Zhu, Yanyu , Zhang, Jing , Zhao, Yan and You, Wansheng(2007) 'Hydrothermal synthesis and crystal structures of two new divalent metal phosphonates with layered structure', *Journal of Coordination Chemistry*, 60: 19, 2075 – 2083, First published on: 29 June 2007 (iFirst)

To link to this Article: DOI: 10.1080/00958970701239572

URL: <http://dx.doi.org/10.1080/00958970701239572>

PLEASE SCROLL DOWN FOR ARTICLE

Full terms and conditions of use: <http://www.informaworld.com/terms-and-conditions-of-access.pdf>

This article may be used for research, teaching and private study purposes. Any substantial or systematic reproduction, re-distribution, re-selling, loan or sub-licensing, systematic supply or distribution in any form to anyone is expressly forbidden.

The publisher does not give any warranty express or implied or make any representation that the contents will be complete or accurate or up to date. The accuracy of any instructions, formulae and drug doses should be independently verified with primary sources. The publisher shall not be liable for any loss, actions, claims, proceedings, demand or costs or damages whatsoever or howsoever caused arising directly or indirectly in connection with or arising out of the use of this material.

Hydrothermal synthesis and crystal structures of two new divalent metal phosphonates with layered structure

LEI MENG, ZHENGANG SUN*, DAPENG DONG, HUI CHEN, YANYU ZHU,
JING ZHANG, YAN ZHAO and WANSHENG YOU

Faculty of Chemistry and Chemical Engineering, Institute of Chemistry for Functionalized Materials, Liaoning Normal University, Dalian, 116029, P. R. China

(Received 18 October 2006; in final form 6 December 2006)

Two divalent metal phosphonates with a layered structure, $\text{Zn}(\text{H}_2\text{L})$ (**1**) and Cd_2L (**2**) ($\text{H}_4\text{L} = \text{CH}_3\text{CH}_2\text{CH}_2\text{N}(\text{CH}_2\text{PO}_3\text{H}_2)_2$), have been hydrothermally synthesized and characterized by single-crystal X-ray diffraction as well as with infrared spectroscopy, elemental analysis and thermogravimetric analysis. The structure of **1** shows a layered structure in which the 1D zinc(II) phosphonate chains are interconnected by bridging organic groups to form 2D layers. In **2**, the interconnection of $[\text{CdO}_5\text{N}]$ and $[\text{CdO}_5]$ polyhedra *via* edge-sharing forms a dimer. The dimers are interconnected by $[\text{CPO}_3]$ tetrahedra *via* corner-sharing to form 2D double layers in the *bc*-plane.

Keywords: Metal phosphonates; Crystal structure; Hydrothermal synthesis; Zinc(II); Cadmium(II)

1. Introduction

The chemistry of metal phosphonates has attracted much attention because of their potential applications in catalysis, ion exchange, proton conductivity, intercalation chemistry, photochemistry, and materials chemistry [1–6]. In recent years, the use of bifunctional or multifunctional anionic units, such as diphosphonates, aminophosphonates or phosphonocarboxylates, has led to new materials with layered or porous structures [7–9]. The layered or porous structures formed by these bi- and multifunctional phosphonic acids are particularly interesting. The metal atoms in these structures are coordinated by the oxygen atoms of the $-\text{PO}_3$ group and a donor atom (usually oxygen or nitrogen) of the group at the other end of an alkyl chain.

The use of the aminodiphosphonic acid, $\text{RN}(\text{CH}_2\text{PO}_3\text{H}_2)_2$ in the synthesis of metal phosphonates has resulted in the formation of 2D or 3D open-frameworks [10–13]. For instance, $\text{Cd}(\text{H}_3\text{L})_2$ ($\text{H}_4\text{L} = \text{C}_6\text{H}_5\text{CH}_2\text{N}(\text{CH}_2\text{PO}_3\text{H}_2)_2$) features double chains that are further interlinked by hydrogen bonds [14]. $\text{Zn}_3(\text{HL})_2$ ($\text{H}_4\text{L} = \text{CH}_3\text{N}(\text{CH}_2\text{PO}_3\text{H}_2)_2$) has a 3D network structure built from $[\text{ZnO}_4]$ tetrahedra linked together by bridging phosphonate groups [15]. To the best of our knowledge, reports on metal phosphonates based on alkyl-substituted aminodiphosphonates are rare. In order to understand the

*Corresponding author. Tel.: +86-411-82156568. Fax: +86-411-82156858. Email: szg188@163.com

effect of the substituent *R* group on the structure of metal phosphonates, we have also been interested in exploring novel metal phosphonate compounds based on alkyl-substituted aminodiphosphonic acids, $\text{RN}(\text{CH}_2\text{PO}_3\text{H}_2)_2$. In this article, we report the synthesis, crystal structure, and thermal stability of two new divalent metal aminodiphosphonates $\text{Zn}(\text{H}_2\text{L})$ (**1**) and Cd_2L (**2**) containing $\text{CH}_3\text{CH}_2\text{CH}_2\text{N}(\text{CH}_2\text{PO}_3\text{H}_2)_2$ (H_4L) with a layered structure.

2. Experimental

2.1. Materials and methods

The aminodiphosphonic acid, $\text{CH}_3\text{CH}_2\text{CH}_2\text{N}(\text{CH}_2\text{PO}_3\text{H}_2)_2$, was prepared by a Mannich type reaction according to procedures previously described [16]. All other chemicals were used as obtained without further purification. C, H and N were determined by using a PE-2400 elemental analyzer. Zn, Cd and P were determined by using an inductively coupled plasma (ICP) atomic absorption spectrometer. IR spectra were recorded on a Bruker AXS TENSOR-27 FT-IR spectrometer with KBr pellets in the range $4000\text{--}400\text{ cm}^{-1}$. TG and DTA analysis were performed on a Perkin–Elmer Pyris Diamond TG-DTA thermal analysis system in static air with a heating rate of 10 K min^{-1} from 50 to 900°C .

2.2. Synthesis of $\text{Zn}(\text{H}_2\text{L})$ (**1**)

A mixture of $\text{Zn}(\text{CH}_3\text{COO})_2 \cdot 2\text{H}_2\text{O}$ (0.11 g, 0.5 mmol), $\text{CH}_3\text{CH}_2\text{CH}_2\text{N}(\text{CH}_2\text{PO}_3\text{H}_2)_2$ (0.25 g, 1 mmol) and water (15.0 mL, 833 mmol) in the mole ratio of 1.0:2.0:1666 was sealed into a 23 mL Teflon-lined stainless steel autoclave and heated at 180°C for 5 days under autogenous pressure. After the mixture cooled slowly to room temperature, colorless block crystals were filtered off, washed with distilled water, and dried at room temperature (Yield: 0.06 g, 38.7% based on Zn). Anal. Calcd for **1**, $\text{C}_5\text{H}_{13}\text{NO}_6\text{P}_2\text{Zn}$ (%): C, 19.34; H, 4.22; N, 4.51; P, 19.95; Zn, 21.06. Found: C, 19.12; H, 4.08; N, 4.68; P, 19.86; Zn, 21.18. Selected IR bands ($4000\text{--}400\text{ cm}^{-1}$ region): 3440, 3039, 2968, 2777, 1630, 1160, 1111, 945, 590, 536, 447.

2.3. Synthesis of Cd_2L (**2**)

A mixture of $\text{Cd}(\text{CH}_3\text{COO})_2 \cdot 2\text{H}_2\text{O}$ (0.13 g, 0.5 mmol), $\text{CH}_3\text{CH}_2\text{CH}_2\text{N}(\text{CH}_2\text{PO}_3\text{H}_2)_2$ (0.25 g, 1 mmol), NaF (0.08 g, 2 mmol) and water (10.0 mL, 555 mmol) in the mole ratio 1.0:2.0:4.0:1110 was sealed into a 23 mL Teflon-lined stainless steel autoclave and heated at 180°C for 5 days. After the mixture cooled slowly to room temperature, colourless needle crystals were filtered off, washed with distilled water, and dried at room temperature (Yield: 0.05 g, 42.7% based on Cd). Anal. Calcd for **2**, $\text{C}_5\text{H}_{11}\text{NO}_6\text{P}_2\text{Cd}_2$ (%): C, 12.83; H, 2.37; N, 2.99; P, 13.24; Cd, 48.05. Found: C, 12.68; H, 2.45; N, 2.78; P, 13.35; Cd, 47.93. Selected IR bands ($4000\text{--}400\text{ cm}^{-1}$ region): 3440, 2949, 2866, 1631, 1460, 1169, 1124, 1070, 1022, 968, 626, 577, 532.

2.4. Crystal structure determinations of **1** and **2**

Suitable single crystals for **1** and **2** were glued to a thin glass fibre and mounted on a Bruker Smart APEX II X-diffractometer equipped with graphite monochromated

Table 1. Crystal data and structure refinements for compounds **1** and **2**.

Compound	1	2
Empirical formula	C ₅ H ₁₃ NO ₆ P ₂ Zn	C ₅ H ₁₁ NO ₆ P ₂ Cd ₂
Formula weight	310.47	467.89
Crystal size (mm ³)	0.12 × 0.08 × 0.03	0.10 × 0.04 × 0.04
Temperature (K)	295(2)	295(2)
Wavelength (Å)	0.71073	0.71073
Crystal system	Triclinic	Monoclinic
Space group (Å, °, Å ³)	<i>P</i> $\bar{1}$	<i>P</i> 2(1)/ <i>c</i>
<i>a</i>	8.0033(12)	12.973(5)
<i>b</i>	8.8803(13)	6.531(3)
<i>c</i>	9.290(2)	13.241(5)
α	102.182(3)	90
β	111.955(3)	103.300(6)
γ	108.506(2)	90
<i>V</i>	538.34(17)	1091.8(7)
<i>Z</i>	2	4
<i>D</i> _c (g cm ⁻³)	1.915	2.847
Absorption coefficient	2.586	4.198
<i>F</i> (000)	316	888
Theta range for data collection	2.55 to 26.50	3.16 to 26.50
Limiting indices	-8 ≤ <i>h</i> ≤ 10, -11 ≤ <i>k</i> ≤ 11, -11 ≤ <i>l</i> ≤ 11	-16 ≤ <i>h</i> ≤ 15, -8 ≤ <i>k</i> ≤ 8, -8 ≤ <i>l</i> ≤ 6
Reflections collected	3200	6150
Independent reflections	2183 [<i>R</i> _{int} = 0.0223]	2260 (<i>R</i> _{int} = 0.0329)
Completeness to $\theta = 26.50$	97.8%	99.6%
Absorption correction	Empirical	Empirical
Max. and min. transmission	0.9218 and 0.7518	0.8568 and 0.6741
Refinement method	Full-matrix least-squares on <i>F</i> ²	Full-matrix least-squares on <i>F</i> ²
Goodness-of-fit on <i>F</i> ²	1.032	1.006
Final <i>R</i> indices [<i>I</i> > 2 σ (<i>I</i>)]	<i>R</i> ₁ = 0.0409 <i>wR</i> ₂ = 0.0859	<i>R</i> ₁ = 0.0262, <i>wR</i> ₂ = 0.0520
<i>R</i> indices (all data)	<i>R</i> ₁ = 0.0580, <i>wR</i> ₂ = 0.0969	<i>R</i> ₁ = 0.0344, <i>wR</i> ₂ = 0.0553

$$R_1 = \Sigma(|F_o| - |F_c|) / \Sigma |F_o|; wR_2 = [\Sigma w(|F_o| - |F_c|)^2 / \Sigma wF_o^2]^{1/2}.$$

Mo-K α radiation ($\lambda = 0.71073 \text{ \AA}$) at $293 \pm 2 \text{ K}$. A hemisphere of intensity data was collected with ω -scans, in the range of $2.55^\circ \leq \theta \leq 26.50^\circ$ for **1** and $3.16^\circ \leq \theta \leq 26.50^\circ$ for **2**. An empirical absorption correction was applied using the SADABS program. The structures were solved by direct methods and refined by full-matrix least squares fitting on *F*² by SHELXTL-97 [17, 18]. All non-hydrogen atoms were refined anisotropically. Hydrogen atoms of organic ligands were generated geometrically with fixed isotropic thermal parameters, and included in the structure factor calculations. The final Fourier map had a minimum and maximum electron density of -0.465 and 0.614 e \AA^{-3} for **1**, and -0.668 and 0.665 e \AA^{-3} for **2**. Summaries of crystal data and structure refinements for the two compounds are listed in table 1. Selected bond lengths and angles are given in table 2.

3. Results and discussion

3.1. Crystal structure

The two compounds have layered structures. However, their layered architectures are different due to different coordination modes of the diphosphonate anion and different coordination geometry around the metal ions.

Table 2. Selected bond lengths (Å) and angles (°) for **1** and **2**.

1			
Zn(1)–O(2)	1.931(3)	Zn(1)–O(4)#2	1.935(3)
Zn(1)–O(1)#3	1.952(3)	Zn(1)–O(6)#1	1.902(3)
P(1)–O(1)	1.498(3)	P(2)–O(6)	1.501(3)
P(1)–O(2)	1.497(3)	P(2)–O(4)	1.509(3)
P(1)–O(3)	1.545(3)	P(2)–O(5)	1.526(3)
P(1)–C(1)	1.813(4)	P(2)–C(2)	1.834(4)
N(1)⋯O(5)#5	2.760(5)	O(3)⋯O(5)#6	2.487(4)
N(1)–H(1C)⋯O(5)#5	174(3)	O(3)–H(3A)⋯O(5)#6	156.7
O(6)#1–Zn(1)–O(2)	108.60(15)	O(1)–P(1)–C(1)	108.1(2)
O(6)#1–Zn(1)–O(4)#2	114.55(14)	O(2)–P(1)–C(1)	106.32(19)
O(2)–Zn(1)–O(4)#2	105.37(14)	O(3)–P(1)–C(1)	101.86(19)
O(6)#1–Zn(1)–O(1)#3	107.74(15)	O(6)–P(2)–O(4)	114.91(19)
O(2)–Zn(1)–O(1)#3	108.41(14)	O(6)–P(2)–O(5)	113.1(2)
O(4)#2–Zn(1)–O(1)#3	111.97(13)	O(4)–P(2)–O(5)	112.00(18)
O(1)–P(1)–O(2)	116.9(2)	O(6)–P(2)–C(2)	103.48(19)
O(1)–P(1)–O(3)	112.88(18)	O(4)–P(2)–C(2)	107.2(2)
O(2)–P(1)–O(3)	109.52(19)	O(5)–P(2)–C(2)	105.14(19)
2			
Cd(1)–O(1)	2.330(3)	Cd(2)–O(1)	2.207(3)
Cd(1)–O(3)#3	2.338(3)	Cd(2)–O(2)#5	2.202(3)
Cd(1)–O(4)	2.355(3)	Cd(2)–O(3)#4	2.280(3)
Cd(1)–O(4)#1	2.279(3)	Cd(2)–O(5)#4	2.162(3)
Cd(1)–O(6)#2	2.282(3)	Cd(2)–O(6)#1	2.298(3)
Cd(1)–N(1)	2.430(4)		
O(4)#1–Cd(1)–O(6)#2	82.91(10)	O(5)#4–Cd(2)–O(2)#5	85.21(12)
O(4)#1–Cd(1)–O(1)	85.19(10)	O(5)#4–Cd(2)–O(1)	110.41(12)
O(6)#2–Cd(1)–O(1)	110.84(10)	O(2)#5–Cd(2)–O(1)	104.33(11)
O(4)#1–Cd(1)–O(3)#3	92.81(11)	O(5)#4–Cd(2)–O(3)#4	90.54(11)
O(6)#2–Cd(1)–O(3)#3	72.31(10)	O(2)#5–Cd(2)–O(3)#4	141.03(11)
O(1)–Cd(1)–O(3)#3	175.97(10)	O(1)–Cd(2)–O(3)#4	113.37(11)
O(4)#1–Cd(1)–O(4)	101.68(6)	O(5)#4–Cd(2)–O(6)#1	145.27(12)
O(6)#2–Cd(1)–O(4)	168.96(10)	O(2)#5–Cd(2)–O(6)#1	88.86(10)
O(1)–Cd(1)–O(4)	79.72(10)	O(1)–Cd(2)–O(6)#1	104.21(11)
O(3)#3–Cd(1)–O(4)	97.29(10)	O(3)#4–Cd(2)–O(6)#1	73.09(10)
O(4)#1–Cd(1)–N(1)	162.13(11)		
O(6)#2–Cd(1)–N(1)	97.95(11)		
O(1)–Cd(1)–N(1)	77.81(11)		
O(3)#3–Cd(1)–N(1)	104.49(11)		
O(4)–Cd(1)–N(1)	80.80(11)		

Symmetry transformations used to generate equivalent atoms: For **1**: #1 $x+1, y+1, z$; #2 $-x+1, -y+1, -z+1$; #3 $-x+2, -y+1, -z+1$; #4 $x-1, y-1, z$; #5 $-x, -y, -z$; #6 $x+1, y, z$. For **2**: #1 $-x, y-1/2, -z+3/2$; #2 $x, y-1, z$; #3 $x, -y+1/2, z-1/2$; #4 $-x, -y+1, -z+2$; #5 $-x, -y, -z+2$; #6 $x, -y+1/2, z+1/2$; #7 $-x, y+1/2, -z+3/2$; #8 $x, y+1, z$.

As shown in figure 1, **1** contains 15 non-hydrogen atoms in the asymmetric unit containing one zinc(II) ion and one partially deprotonated H₂L anion. The Zn–O bond lengths are in the range 1.902(3)–1.952(3) Å, comparable to those reported for other Zn(II) aminodiphosphonates [13, 15]. The zinc(II) is tetrahedrally coordinated by four phosphonate oxygen atoms from four separate H₂L ligands. The aminodiphosphonate ligand acts as a tetradentate metal linker, and bridges four Zn(II) ions. Based on the charge balance, the aminodiphosphonate anion is 2– in charge, and the amine group and O3 remain protonated.

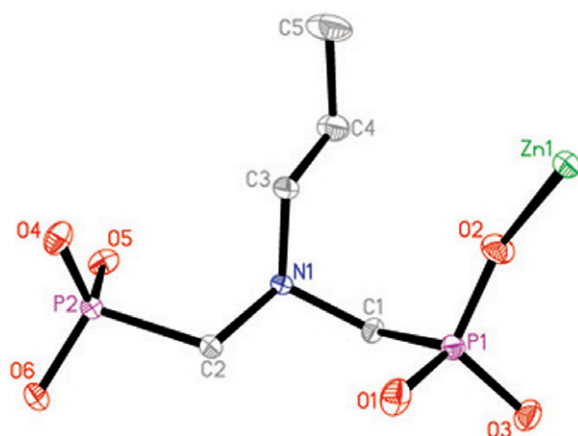


Figure 1. Asymmetric unit of **1** showing the atom labeling. Thermal ellipsoids are shown at the 30% probability level.

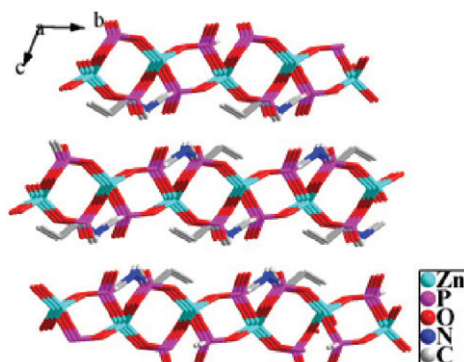


Figure 2. View of the 2D layered structure of compound **1** along the a -axis.

Compound **1** can be described as a 2D layered structure with channels running along the a axis (figure 2). The corner-sharing connections of the alternating $[\text{ZnO}_4]$ and $[\text{CPO}_3]$ tetrahedra result in a zinc phosphonate chain along the b -axis, and adjacent chains are linked through the $-\text{C}-\text{N}-\text{C}-$ chain of $-\text{CH}_2-\text{NH}(\text{C}_3\text{H}_7)-\text{CH}_2-$ to form a layered structure in the ab plane (figure 3a). The result of cross-linking chains in this manner is the formation of two types of rings. One is eight-member rings assembled with the sequences $\text{Zn}-\text{O}-\text{P}-\text{O}-\text{Zn}-\text{O}-\text{P}-\text{O}$ (figure 3b), and the other is 16 member rings formed by 2 H_2L and 2 Zn ions (figure 3c). The propyl groups of the ligands are orientated toward the cavity created by the 16-membered rings as shown in figure 3(a). Between two adjacent layers, the protonated nitrogen atom N1 forms a hydrogen bond with the non-coordinated phosphonate oxygen, O5. The hydrogen bond $\text{N1}-\text{H1C}\cdots\text{O5}$ (symmetry code: $-x, -y, -z$) has a $\text{D}\cdots\text{A}$ distance of $2.760(5)$ Å and $\text{D}-\text{H}\cdots\text{A}$ angle of $147(3)^\circ$.

Compound **2** consists of two crystallographically independent $\text{Cd}(\text{II})$ ions and one fully deprotonated L anion in its asymmetric unit (figure 4). Cd1 is octahedrally coordinated by a L ligand in a tridentate fashion (N1, O1 and O4) and three oxygen

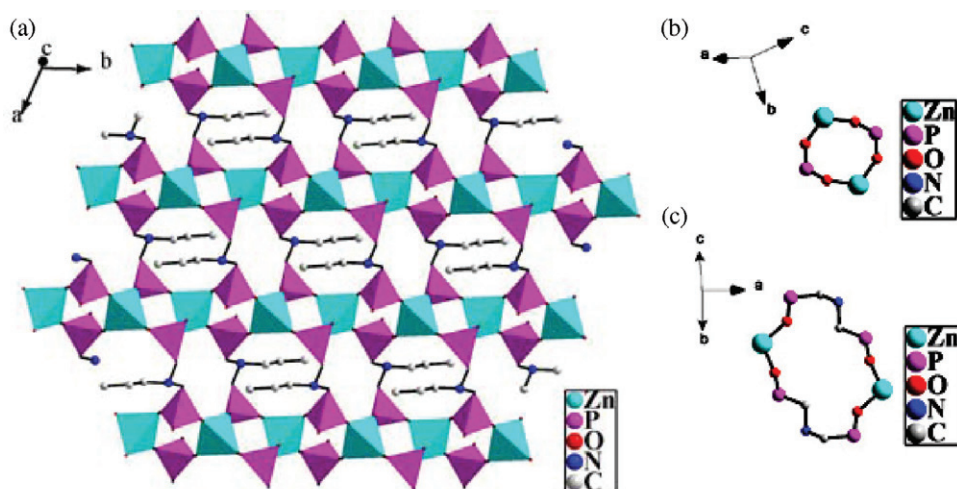


Figure 3. (a) Polyhedral representation of a Zn(II) phosphonate layer for compound **1** in *ab*-plane. (b) One eight-membered ring assembled with the sequences Zn–O–P–O–Zn–O–P–O. (c) One 16-membered ring formed by 2L ligands and 2 Zn atoms.

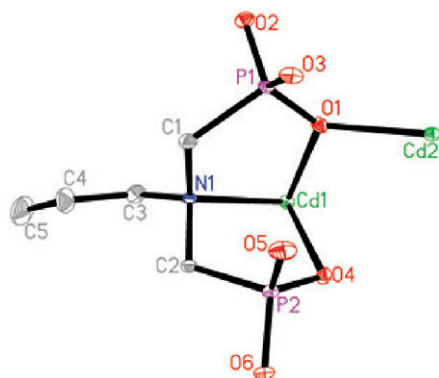


Figure 4. Asymmetric unit of **2** showing the atom labeling. Thermal ellipsoids are shown at the 30% probability level.

atoms from three neighboring Cd_2L units. Cd_2 is coordinated by five phosphonate oxygen atoms from four separate L ligands to form a distorted square pyramid.

The Cd–O distances range from 2.162(3) to 2.355(3) Å, and the Cd–N distance is 2.430(4) Å. These values are in agreement with those reported for other Cd(II) aminodiphosphonates [14, 19]. In the L anion all six phosphonate oxygen atoms and nitrogen atom of the amine group are involved in metal coordination.

The interconnection of $[\text{CdO}_5\text{N}]$ and $[\text{CdO}_5]$ polyhedra *via* edge-sharing forms a dimer. The dimers are interconnected by $[\text{CPO}_3]$ tetrahedra *via* corner-sharing to form 2D double layers in the *bc*-plane (figure 5). The interlayer distance is ca 12.97 Å. The propyl groups of the ligands are oriented toward the interlayer space as shown in figure 6.

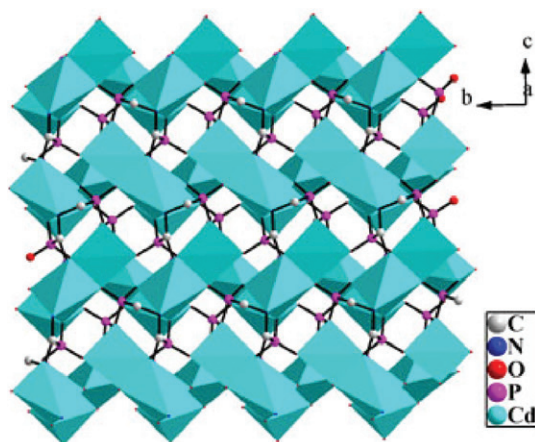


Figure 5. A ball-and-stick and polyhedral representation of a Cd(II) phosphonate layer for **2** in the bc -plane. The propyl groups of the ligands have been omitted for clarity.

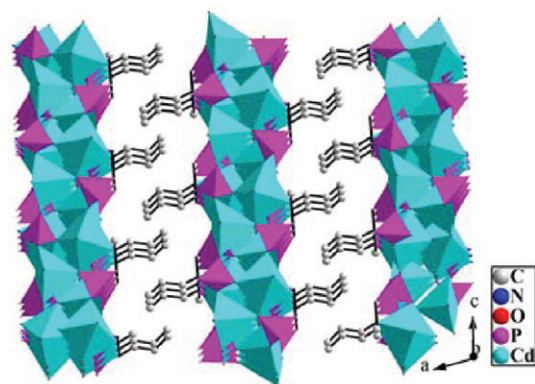


Figure 6. View of the structure of **2** along the b -axis. $[\text{CdO}_5\text{N}]$ and $[\text{CdO}_5]$ polyhedra are shaded in cyan, and $[\text{CPO}_3]$ tetrahedra are shaded in purple. The propyl groups of the ligands are oriented towards the interlayer space.

3.2. IR spectra

The IR spectra were recorded between 4000 and 400 cm^{-1} . The wide band at 3440 cm^{-1} for compound **1** can be assigned to the O–H stretching vibration of the hydrogen bonds [14]. The sharp bands at 2968 cm^{-1} for **1** and 2949 cm^{-1} for **2** are due to the CH_2 stretching vibrations. The bands around 3400 cm^{-1} and one sharp band at 1631 cm^{-1} for **2** are characteristic of the amine coordinated to the metal atom. The band at 2777 cm^{-1} for **1** can be attributed to $\nu(\text{P-OH})$, characteristic of hydrogen phosphonate groups. The set of bands between 1200 and 900 cm^{-1} is due to stretching vibrations of the tetrahedral C– PO_3 groups.

3.3. Thermogravimetric analysis

The TGA diagram of **1** shows thermal stability to 330°C (figure 7a). Above this temperature, a continuous weight loss was observed up to 800°C , corresponding

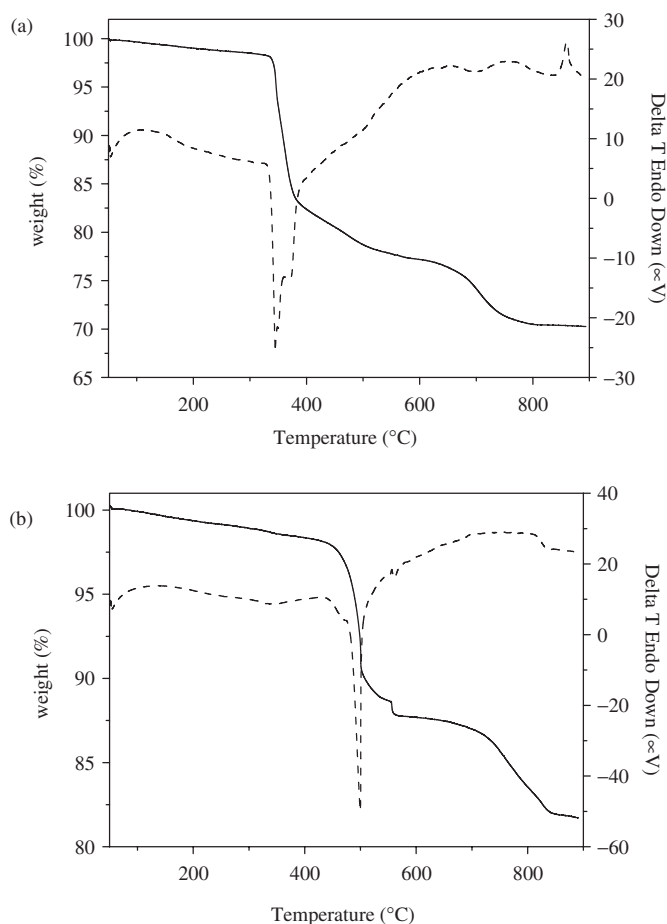


Figure 7. The TG-DTA curves of **1** and **2**.

to pyrolysis of the organic group. The total mass loss (27.7%) is close to the calculated one of 28.1% if the final product is assumed to be $\text{Zn}(\text{PO}_3)_2$. The DTA curve exhibits one endothermic peak at approximately 345°C, corresponding to decomposition of the organic groups. The TGA diagram of **2** indicates two main weight losses (figure 7b). The first step started at 450°C and ended at 720°C, during which the organic groups were burnt. The second weight loss occurred above 720°C, corresponding to further decomposition of the compound. The total weight loss of 15.7% is close to the calculated value (14.8%). The DTA curve exhibits one endothermic peak at approximately 500°C, corresponding to decomposition of the organic groups. The final product is assumed to be $\text{Cd}_2\text{P}_2\text{O}_7$.

Supplementary material

Crystallographic data for compounds **1** and **2** reported in this article have been deposited with the Cambridge Crystallographic Data centre, CCDC Number 611975

for **1** and 611977 for **2**. Copies of this information may be obtained free of charge from The Director, CCDC, 12 Union Road, Cambridge, CB21EZ, UK (Fax: +44-1223-336-033; Email: deposit@ccdc.cam.ac.uk).

Acknowledgement

This work was supported by grants from the Natural Science Foundation of Liaoning Province of China (20062140) and the Education Department of Liaoning Province of China (05L214).

References

- [1] A. Clearfield, Metal phosphonate chemistry. In *Progress in Inorganic Chemistry*, K.D. Karlin (Ed.), Vol. 47, p. 371 (1998), and references therein.
- [2] A. Clearfield. *Curr. Opin. Solid State Mater. Sci.*, **1**, 268 (1996).
- [3] G. Alberti, U. Costantino. In *Comprehensive Supramolecular Chemistry*, J.M. Lehn (Ed.), pp. 1, 15, Pergamon-Elsevier Science Ltd, London (1996).
- [4] M.E. Thompson. *Chem. Mater.*, **6**, 1168 (1994).
- [5] A. Clearfield. *Chem. Mater.*, **10**, 2801 (1998).
- [6] K. Maeda. *Micropor. Mesopor. Mater.*, **73**, 47 (2004).
- [7] K. Barthelet, D. Riou, G. Ferey. *Solid State Sci.*, **4**, 841 (2002).
- [8] A. Clearfield, C.V.K. Sharma, B. Zhang. *Chem. Mater.*, **13**, 3099 (2001).
- [9] B. Zhang, A. Clearfield. *J. Am. Chem. Soc.*, **119**, 2751 (1997).
- [10] J.G. Mao, Z.K. Wang, A. Clearfield. *Inorg. Chem.*, **41**, 6106 (2002).
- [11] P.L. Gentili, U. Costantino, M. Nocchetti, C. Miliani, G. Favaro. *J. Mater. Chem.*, **12**, 2872 (2002).
- [12] S.M. Ying, X.R. Zeng, X.N. Fang, X.F. Li, D.S. Liu. *Inorg. Chim. Acta.*, **359**, 1589 (2006).
- [13] J.G. Mao, Z.K. Wang, A. Clearfield. *New J. Chem.*, **25**, 1010 (2002).
- [14] Z.M. Sun, B.P. Yang, Y.Q. Sun, J.G. Mao, A. Clearfield. *J. Solid State Chem.*, **176**, 62 (2003).
- [15] J.G. Mao, A. Clearfield. *Inorg. Chem.*, **41**, 2334 (2002).
- [16] K. Moedritzer, R.R. Irani. *J. Org. Chem.*, **31**, 1603 (1966).
- [17] G.M. Sheldrick. *SHELXTL-97, Program for Crystal Structure Solution*, University of Göttingen, Germany (1997).
- [18] G.M. Sheldrick. *SHELXTL-97, Program for Crystal Structure Refinement*, University of Göttingen, Germany (1997).
- [19] J.G. Mao, Z.K. Wang, A. Clearfield. *Inorg. Chem.*, **41**, 3713 (2002).